DNA Charge Neutralisation by Linear Polymers II: Reversible Binding

E. Maltsev,* J. A. D. Wattis,† and H. M. Byrne‡
Centre for Mathematical Medicine,
School of Mathematical Sciences,
University Park, University of Nottingham,
Nottingham, NG7 2RD, UK

We model the way in which polymers bind to DNA and neutralise its charged backbone by analysing the dynamics of the distribution of gaps along the DNA. We generalise existing theory for irreversible binding to construct new deterministic models which include polymer removal, movement along the DNA and allow for binding with overlaps. We show that reversible binding alters the capacity of the DNA for polymers by allowing the rearrangement of polymer positions over a longer timescale than when binding is irreversible. When the polymers do not overlap, allowing reversible binding increases the number of polymers adhered and hence the charge that the DNA can accommodate; in contrast, when overlaps occur, reversible binding reduces the amount of charge neutralised by the polymers.

PACS numbers: 82.20.-w, 82.30.-b, 82.39.-k, 05.90.+m,89.75.Fb

I. INTRODUCTION

In this paper we extend a deterministic mathematical model of polymer binding [1] to include removal and movement of polymers along the DNA plasmid. Both the kinetics of reversible binding and the steady state (equilibrium) solutions are studied. The DNA is modelled as a single one-dimensional strand, with uniformly spaced binding sites. The model is used to analyse how the distribution of gap sizes evolves when polymers attach to the DNA. Such knowledge allows us to calculate the fraction of DNA sites occupied by the polymers and the resulting charge neutralisation.

The resulting model has the form of a generalised 'parking problem', also known as 'Random Sequential Absorption', (RSA) and has been studied by Rényi [2] and Bonnier *et al.* [3]. Epstein [4, 5] has applied the RSA model to polymer absorption, where it is referred to as 'the excluded site binding model' and has been used to estimate the time variation of charge neutralisation, as well as the equilibrium value [6]. One area where knowledge of charge neutralisations is vital is in the delivery of gene therapy. The successful introduction of DNA into the nucleus of an abnormal cell requires the DNA to be compacted: one way of achieving this is through the use of cationic polymers [7].

A recent review of RSA models is given by Talbot *et al.* [8]. Whilst this describes the generalisation of RSA to the adsorbtion of particles with a variety of shapes and a range of sizes to a surface, the problem of reversibile binding is only briefly addressed. Exact solutions and large-time asymptotic results of RSA systems have been derived by Ben-Naim & Krapivsky [9], who also consider generalised RSA models which include reversible binding (Krapivsky & Ben-Naim [10]). Both Brewer *et al.* [11, 12] and Lever *et al.* [13] show that DNA condensation by polymers is a reversible process. Tarjus *et al.* [14] analyses a generalised RSA model in which either binding and desorption or binding and surface diffusion of polymer on DNA occurs. Although complex, the model is analysed theoretically in the low coverage limit. This contrasts with our results for an alternative generalised RSA model with reversible binding and surface diffusion of adsorbed polymers, where asymptotic results are obtained for the high coverage regime. Other extensions of RSA to include cooperative effects have been studied by Evans [15], and Barma [16]; the latter including diffusion of adsorbed particles along the substrate. Van Tassel *et al.* [17] also present a generalised model of partially reversible RSA. In the spirit of Michaelis-Menten reaction kinetics, they assume that upon binding to a substrate, the polymer which is in its native state and the substrate form a metastable complex. It is possible for this complex to unbind, or for the polymer to undergo some conformational change in which it becomes irreversibly bound to the substrate. They argue that such a model is more accurate than Langmuir-models due to the treatment of surface blocking.

Teif [18] models polymer adsorption to DNA with different on and off rates for normal and condensed DNA and incorporates the effect of dissolved salt on the condensation process. His models explain decondensation of the DNA at very high polymer concentrations through resolubilisation of the DNA. The cooperativity parameter in the McGhee-von Hippel model can be motivated by the fact that some polymers have sticky ends and free polymer is more likely to bind adjacent to an already-

*Electronic address: Eugene.Maltsev@maths.nottingham.ac.uk
†Corresponding Author; Electronic address: Jonathan.Wattis@nottingham.ac.uk
‡Electronic address: Helen.Byrne@nottingham.ac.uk

bound polymer than in the interior of a gap. However, many condensing polymers do not have sticky ends yet still exhibit a cooperative binding effect, so an alternative justification is required. Brewer *et al.* [11] shows that for DNA condensation into toroids by adsorption of protamine, polymer adhesion is the rate-limiting step in condensation. If condensation occurs immediately upon polymer binding; then the DNA will locally change its shape at and near the region of bound polymers; this provides a mechanism for the rates of polymer attachment and removal to differ near already bound polymers from those in uncondensed DNA.

The remainder of this section contains an introduction to the notation we use to derive our models of polymer-adherence to DNA, and a summary of the results obtained in [1] for irreversible binding with and without overlaps. In Section I A we summarise the modelling approach and quote the model for irreversible binding, the gap distribution kinetics for reversible binding are derived in Section II. A corresponding model for partially-overlapping polymers is derived in Section III; this model allows charge inversion [19], this occurs when so much polymer adheres to the DNA that the complex acquires a positive charge. The model is extended to include polymer motion along the DNA in Section IV. Even though the dynamic model is slow to solve numerically when motion is included, the asymptotic solutions for fast motion allow us to calculate the charge neutralisation associated with polymer binding with or without motion (see Section IV B) and our asymptotic solution method is applied to find steady state solutions in Section IV C. Reversible binding of overlapping polymers with motion is studied in Section V. The results are discussed in Section VI.

A. Modelling approach

Here, we follow the modelling approach introduced in [1]. We define x to be the length of the polymer, and p to be the length of the gap in which the incoming polymer will bind. Both x and p are integers, and for the case of charged polymers binding to DNA they represent numbers of base pairs. We define $N_p(t)$ to be the number of gaps of length p at time t. In the simpler cases only positive gap lengths are considered, however, we show later that binding with overlaps can be incorporated into such models by treating overlaps as gaps with negative lengths.

The length of the DNA molecule is P_0 (each site corresponds to a negatively charged phosphate group) and the concentration of the DNA is measured in moles (M) and denoted by A_0. The following parameters (with corresponding units) are used: binding, removal and movement rates k_f ($\mathrm{s}^{-1}\mathrm{M}^{-1}$), k_r (s^{-1}) and k_m (sites$\times\mathrm{s}^{-1}$) respectively; the concentrations of bound, and free polymers in solution are B (M) and L (M) respectively; L_0 (M) denotes the initial number of polymers in solution (so $B = L_0 - L$). The notation for the length, rates and concentrations is summarised in Figure 1.

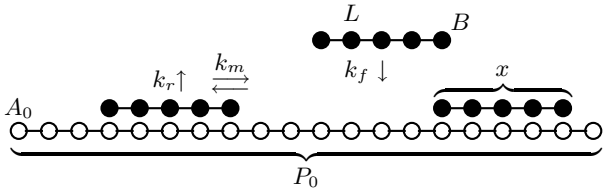

FIG. 1: Summary of polymer binding notation for a case when $A_0 = 1$, $P_0 = 20$, $x = 5$, $L_0 = 3$, $L = 1$ and $B = 2$.

As polymers adhere, they neutralise the negative charge of the DNA; however we ignore the electrostatic-thermodynamic properties of the system in favour of a model which is more faithful to the geometric constraints of binding and blocking of binding sites. Our model is thus more closely related to models of random sequential adsorption rather than the counterion condensation theories of Manning [20] and Rouzina & Bloomfield [21]. Two physical quantities derived from the gap size distribution can be used to calculate the extent of charge neutralisation. They are the total number of gaps, M_0, as defined by

$$M_0(t) = \sum_{p=0}^{P_0} N_p(t), \tag{1}$$

and the total length of gaps, M_1,

$$M_1(t) = \sum_{p=1}^{P_0} pN_p(t). \tag{2}$$

The charge neutralisation θ is defined to be the proportion of charges on the DNA neutralised by the polymer. This can be calculated in two ways

$$\theta(t) = \frac{x\,(M_0(t) - 1)}{P_0} = \frac{P_0 - M_1(t)}{P_0}, \tag{3}$$

since $M_0 - 1$ is the number of polymer molecules attached to the DNA plasmid and $P_0 - M_1$ is the total number of sites occupied by the polymers. Thus the identity

$$xM_0(t) + M_1(t) = P_0 + x, \tag{4}$$

is valid for all t.

Since the number of polymers bound to the DNA is $M_0 - 1$, the concentration of bound polymers is $B = A_0(M_0 - 1)$, where A_0 is the molar concentration of DNA. Hence the molar concentration of free polymers $L(t)$ can be expressed in terms of the sum of all gaps as

$$L(t) = L_0 - B(t) = L_0 - A_0(M_0(t) - 1), \tag{5}$$

where $L_0 = L(t = 0)$ is the molar concentration of polymers in the solution before any binding occurs.

The rate at which the gap distribution N_p evolves over time is calculated by considering the rates at which gaps

are created and destroyed during polymer adhesion (F_p), removal (U_p) and movement (V_p) of polymers. Combining the above rates results in

$$\frac{\mathrm{d}N_p}{\mathrm{d}t} = F_p^f - F_p^r + U_p^f - U_p^r + V_p^f - V_p^r, \qquad (6)$$

where f and r in the superscripts refer to the rates at which gaps are formed and removed respectively.

B. Irreversible binding

Irreversible binding without motion occurs when F_p^f and F_p^r are the only non-zero terms in (6). When the irreversible binding terms [1, 22] are separated into gap creation and removal components we have

$$F_p^f = \quad 2K_f \sum_{g=p+x}^{P_0} N_g, \qquad (7a)$$

$$F_p^r = \; K_f(p-x+1)N_p, \qquad (7b)$$

where K_f is the binding rate defined by $K_f = k_f L(t)$, and k_f is a rate constant. The full system of equations for the gap distribution kinetics is

$$\frac{\mathrm{d}N_p}{\mathrm{d}t} = -F_p^r \qquad (P_0-x+1 \le p \le P_0), \qquad (8a)$$

$$\frac{\mathrm{d}N_p}{\mathrm{d}t} = F_p^f - F_p^r \qquad (x \le p \le P_0-x), \qquad (8b)$$

$$\frac{\mathrm{d}N_p}{\mathrm{d}t} = F_p^f \qquad (0 \le p \le x-1). \qquad (8c)$$

See Figure 2(a) for an illustration of gaps formed as polymers bind without overlaps. In [1] the system of equations (8) was solved numerically for a variety of cases. Figure 5 shows how the charge neutralisation $\theta(t)$ defined in equation (3) evolves over time (dashed line). Recurrence relations for the steady-state value of θ are derived, and an asymptotic analysis enables approximate solutions to be constructed. The curve does not asymptote to $\theta = 1$ because the polymers have length $x > 1$, they bind at random positions, and as a result gaps form between bound polymers. When all gaps are smaller than x, no further binding can occur, yet not all of the charges on the DNA have been neutralised. Thus the final charge neutralisation will be below 100%. Guided by experimental work involving long polymers and longer strands of DNA [23], the particular scalings considered are $x \gg 1$ and $P_0 = \mathcal{O}(x^2)$, and in this limit we obtain

$$\theta \sim \frac{3x}{4x-1}\left(1 - \frac{x-1}{3P_0}\right).$$

In Section II, we generalise (8) to allow for polymer-removal and polymer motion along the DNA.

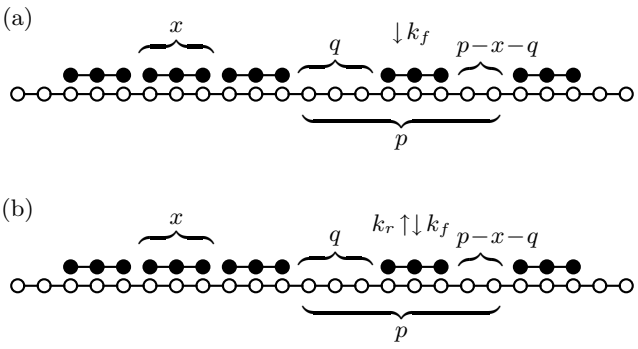

FIG. 2: (a) Illustration of how polymer adhesion destroys a gap of size p and leads to the formation of gaps of length q and $p - x - q$; (b) Illustration of how polymer removal can lead to the formation of a gap of length p, and how polymer adhesion leads to the formation of a gap of length q.

The case of irreversible binding with overlaps is also considered in [1]; here the gap creation and removal components are

$$F_p^f = 2K_f \sum_{g=p+1}^{P_0} N_g, \qquad (9a)$$

$$F_p^{f-} = 2K_f \sum_{g=1}^{P_0} N_g, \qquad (9b)$$

$$F_p^r = K_f(p+x-1)N_p, \qquad (9c)$$

where K_f is the binding rate defined by $K_f = k_f L(t)$, and k_f is a rate constant. Gaps with $p < 0$ describe overlaps of size $-p$, and the new term F_p^{f-} denotes the rate of creation of overlaps. The full system of equations for the gap distribution kinetics is

$$\frac{\mathrm{d}N_{P_0}}{\mathrm{d}t} = -F_{P_0}^r, \qquad (10a)$$

$$\frac{\mathrm{d}N_p}{\mathrm{d}t} = F_p^f - F_p^r \qquad (1 \le p \le P_0 - 1), \qquad (10b)$$

$$\frac{\mathrm{d}N_p}{\mathrm{d}t} = F_p^{f-} \qquad (1-x \le p \le 0). \qquad (10c)$$

In place of (1) and (2) we now have

$$M_0 = \sum_{p=1-x}^{P_0} N_p(t), \qquad M_1 = \sum_{p=1-x}^{P_0} pN_p(t); \qquad (11)$$

with these new definitions, the identity (4) and the formula (3) both still hold.

See Figure 3 for an illustration of polymer binding with overlaps. In Section III (10) is generalised to include polymer motion and removal. Our earlier paper [1] presents the results of numerical simulations of irreversible binding models, together with asymptotic analysis of the system for long DNA plasmids and long polymers. Plots of charge neutralisation over time have the

same sigmoidal shape as the dashed line in Figure 5, although they rise to values between $\theta = 1$ and $\theta = 3$, (see, for example, the solid line in Figure 10). For $x \sim \sqrt{P_0} \gg 1$ asymptotic analysis of the charge neutralisation recurrence relation showed that $\theta \sim 2 - 2/x + x/P_0$. It was also found that at equilibrium, the distribution of overlap sizes is uniform, in contrast with the equilibrium distribution of gap sizes in the non-overlapping case where there are many more smaller gaps.

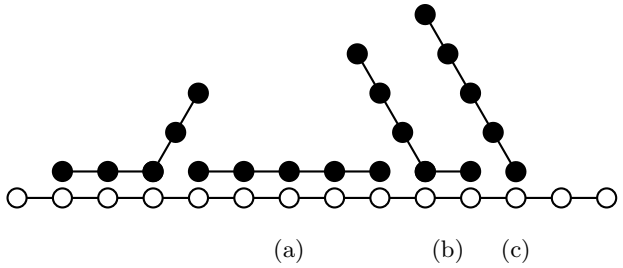

FIG. 3: Polymers of length $x = 5$ with overlaps.

II. NON-OVERLAPPING REVERSIBLE BINDING

In this section we extend the model of non-overlapped binding (8) to incorporate reversible binding, so that in equation (6) $F_p^{f,r}$ and $U_p^{f,r}$ are non-zero but $V_p^{f,r} = 0$. The model is derived in subsection II A and numerical results are presented in II B.

A. Kinetics of gap creation and destruction due to polymer unbinding

A gap of size p is created when a polymer of length x is removed if two gaps of length q and $p - q - x$ are destroyed (see Figure 2(b)): we represent this situation as follows

$$(p - x - q) + (q) \to (p). \tag{12}$$

The frequency at which the shorter gaps occur is proportional to $N_q N_{p-q-x}$. These two gaps have to be separated by a bound polymer. Since the gap N_{p-q-x} could be located in any of M_0 positions, the frequency at which both gaps occur separated by just one bound polymer is

$$\frac{N_q N_{p-q-x}}{M_0}. \tag{13}$$

If the polymers are removed from the DNA at the rate k_r (s^{-1}) then the total number of gaps of length p that are created when (12) occurs is

$$U_p^f = \frac{k_r}{M_0} \sum_{q=0}^{p-x} N_q N_{p-x-q}. \tag{14}$$

With U_p^f defined by (14) we use a similar argument to determine how gaps of length p are destroyed when a polymer is removed from the DNA, and hence specify U_p^r.

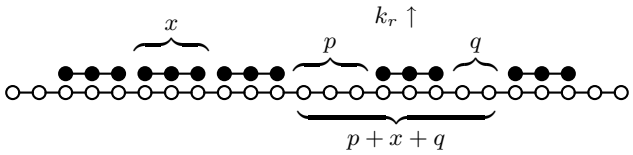

FIG. 4: Illustration of the destruction of a p-gap due to polymer unbinding.

A gap of length p will be destroyed by removal if there is a corresponding gap of length q separated by one bound polymer of length x. In this case, the two gaps (p, q) coalesce to form one larger gap of length $p + x + q$ (see Figure 4):

$$(p) + (q) \to (p + x + q). \tag{15}$$

Adopting the same approach that was used to obtain (14), but noting that two gaps are destroyed whenever a polymer unbinds, we deduce that the rate of gap removal due to polymer unbinding U_p^r is given by

$$U_p^r = \frac{2k_r}{M_0} N_p \sum_{q=0}^{P_0-p-x} N_q. \tag{16}$$

When $P_0 \gg x$, equation (16) can be approximated by

$$U_p^r = 2k_r N_p. \tag{17}$$

The gap creation (14) and destruction (16) terms are combined with (8) to obtain the following differential equations for the kinetics of gap distribution of the non-overlapping reversible binding system

$$\frac{\mathrm{d}N_p}{\mathrm{d}t} = -F_p^r + U_p^f \qquad (P_0 - x + 1 \le p \le P_0), \tag{18a}$$

$$\frac{\mathrm{d}N_p}{\mathrm{d}t} = F_p^f - F_p^r + U_p^f - U_p^r \qquad (x \le p \le P_0 - x), \tag{18b}$$

$$\frac{\mathrm{d}N_p}{\mathrm{d}t} = F_p^f - U_p^r \qquad (0 \le p \le x - 1). \tag{18c}$$

We note that gaps of size $P_0 - x + 1 \le p \le P_0$ cannot be destroyed by polymer-removal and therefore (18a) contains only the gap creation term U_p^f. When polymers leave the DNA, they always create gaps at least as long as the polymer itself. Hence when considering short gaps with $0 \le p \le x - 1$ only gap destruction terms (U_p^r) are present (see (18c)).

B. Numerical solution

The evolution of gap distributions $N_p(t)$ was calculated by solving equations (18) numerically using a semi-explicit interpolation method [24] with adaptive step-size

control written and compiled using Fortran 90. The charge neutralisation was calculated from $\theta = x(M_0 - 1)/P_0$, where M_0 is the total number of gaps (see (3)).

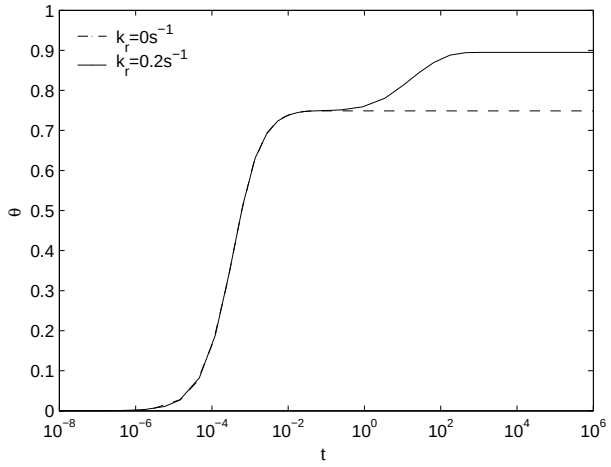

FIG. 5: Curves showing how, for nonoverlapped binding, polymer removal affects the charg neutralisation dynamics $\theta(t)$ and, in particular, increases the equilibrium charge neutralisation. Parameter values: $L_0 = 10^{-6}$ M, $A_0 = 2 \times 10^{-9}$ M, $P_0 = 500$ sites, $x = 20$ sites, $k_f = 10^8 \mathrm{M}^{-1}\mathrm{s}^{-1}$.

When the polymers bind reversibly to the DNA we find a second phase of kinetic behaviour which occurs over a longer timescale, during which the charge neutralisation exceeds that for irreversible binding (see Figures 5, 7 and 8). The initial rise in charge neutralisation is the same for reversible and irreversible binding. That the inclusion of polymer removal causes a later *increase* in charge neutralisation is perhaps counter-intuitive. During this latter phase of the process, polymer desorption allows the rearrangement of polymers on the DNA: polymer removal and reattachment leads to changes in the distribution of gaps sizes. The equilibrium gap distribution corresponding to the charge neutralisation curves shown in Figure 5 is plotted in Figure 6 and shows that reversible binding results in a less uniform distribution of gap-sizes at equilibrium than is the case with irreversible binding. Over the longer timescale, polymer-rearrangement causes an increased frequency of shorter gaps, creating other gaps large enough for extra polymer-landing and hence is consistent with the increased charge neutralisation observed in Figure 5.

1. *Effect of varying the kinetic rates*

The plot in Figure 7 shows the effect on charge neutralisation of varying the binding and removal rates. The first effect to notice is that the time of the initial rise from $\theta = 0$ depends on the rate of binding k_f, the solid and dashed curves are initially coincident ($k_f = 10^{10}$ M^{-1} s^{-1}), as are the dotted and the dash-dotted lines ($k_f = 10^8$ M^{-1} s^{-1}). For the parameter values used, the

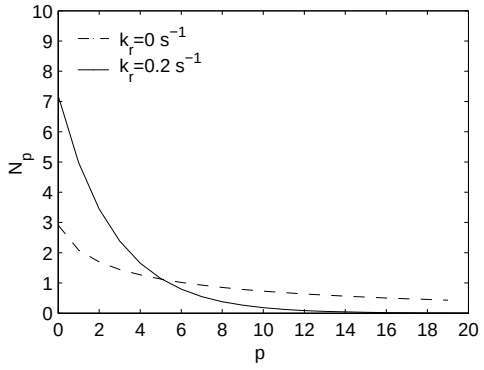

(a) Linear scale

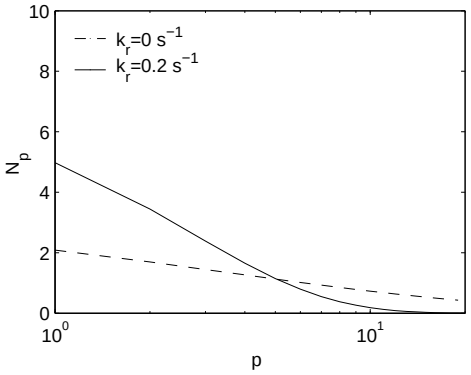

(b) Log scale

FIG. 6: Curves showing how, for non-overlapped binding, polymer removal changes the equilibrium gap distribution. Parameter values are as in Figure 5).

simulations show that the rate of removal does not influence the binding kinetics until θ exceeds one half. (By making the removal rate k_r extremely large, it is possible to make the equilibrium charge neutralisation curve asymptote to a low value of θ).

If $k_r = 0$ the initial plateau is maintained for all subsequent times, however if $k_r > 0$, there is a second phase of kinetics occurring over a longer timescale, in which higher charge neutralisations are accessible as a second plateau in θ is attained. In the case of the dash-dotted line, the removal rate is so large that only one plateau is seen. The height of the final plateau depends on the ratio of the removal and binding rates, thus the dotted curve and the solid curve approach the same limit, with the dotted curve simply being shifted in the horizontal direction, since its rates are simply multiples of those for the solid curve.

When the removal rate is increased, with the binding rate fixed the equilibrium charge neutralisation falls (compare dotted with dash-dotted line). We note also that when only the binding rate is increased and the re-

moval rate fixed then the initial increase in θ occurs earlier and the final equilibrium value of θ is also increased (compare dashed and dotted lines).

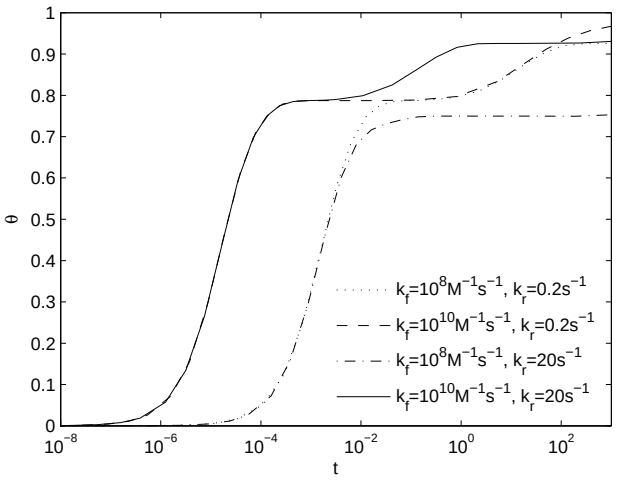

FIG. 7: Series of curves showing how changing the binding and removal rates influences the charge neutralisation dynamics, $\theta(t)$. Parameter values: $L_0 = 10^{-6}$M, $A_0 = 5 \times 10^{-9}$M, $P_0 = 200$ sites, $x = 5$ sites.

2. *Effect of varying the polymer length*

The effect of changing polymer length on charge neutralisation is shown in Figure 8. We find that initially longer polymers adhere at a greater rate, leading to faster kinetics, but that the equilibrium charge neutralisation is lower (compare solid and dashed curves in Figure 8).

There are two phenomena that our model has not yet taken into account. Firstly, since longer polymers have greater charge, their binding and removal rates may differ from those of shorter polymers. Secondly, the initial concentration of polymers was identical in both cases. Therefore in the case of longer polymers, there are more polymeric charges available to neutralise the DNA. Fewer longer polymers are required to cover the DNA surface and hence the reduction in the binding rate will be greater in the case of shorter polymers. One might expect this to promote higher charge neutralisation when longer polymers are used. However, longer polymers also give rise to longer gaps on the DNA plasmid, reducing its charge neutralisation. In practice, the latter effect prevails: thus in Figure 8 the equilibrium value of θ is lower for the longer polymer (compare solid and dashed curves).

L_0x is the total amount of charge in the system. If we increase the polymer length (x) while holding L_0 fixed then this will increase the total amount of polymer charge available to neutralise the DNA. From Figure 8 we note that a simple increase in x, with L_0 fixed, leads to accelerated kinetics, a lower intermediate plateau and a slightly lower equilibrium value of θ. We now investigate the effect of increasing the polymer length (x) and decreasing L_0 so that the total amount of polymer charge (xL_0) is held constant.

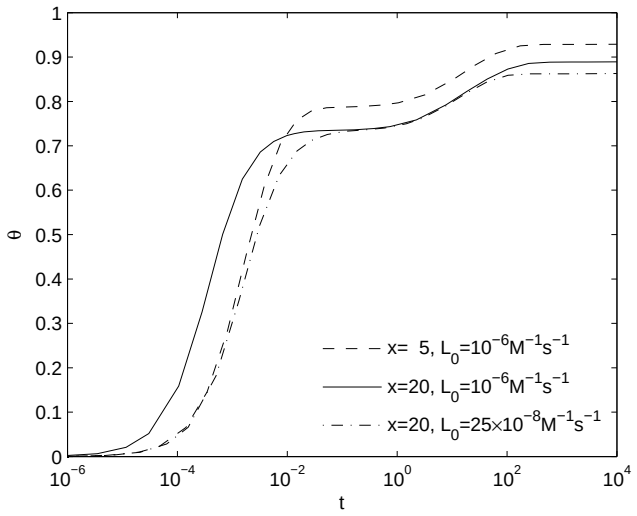

FIG. 8: Series of curves illustrating how the length of the polymer, with adjusted binding rate, affects the charge neutralisation dynamics $\theta(t)$. Parameter values: $A_0 = 5\times10^{-9}$M, $P_0 = 200$ sites, $k_f = 10^8\mathrm{M}^{-1}\mathrm{s}^{-1}$, $k_r = 0.2\mathrm{s}^{-1}$.

Comparing dashed and dot-dashed lines in Figure 8 indicates that an increase in polymer length combined with a reduction in the binding rate (by a factor of four in both cases) results in an approach to the first plateau of the graph on a similar timescale. This corresponds to the equilibrium value of the charge-neutralisation in the irreversible binding case, which is higher for short polymers. Following that, the kinetics of the dash-dotted curve ($x = 20$, $L_0 = 0.25 \times 10^{-6}\mathrm{M}^{-1}\mathrm{s}^{-1}$) are similar to those of the original, 20-site polymer (solid curve, $L_0 = 10^{-6}$) but the reversible binding equilibrium (second plateau) is lower for $L_0 = 0.25\times10^{-6}$ than for $L_0 = 10^{-6}$, indicating a more complex dependence on the polymer length, polymer concentration in the solution, and binding and removal rates.

III. OVERLAPPING REVERSIBLE BINDING

We now generalise the above model of reversible binding to include cases when polymers bind with only some of their charges, leaving ends which overlap with neighbouring bound polymers. The effect can be incorporated into our models quite naturally by describing an overlap of p sites as a gap of size $-p$. This again corresponds to equation (6) with $F_p^{f,r}$ and $U_p^{f,r}$ non-zero and $V_p^{f,r} = 0$.

A. Removal kinetics

Even when negative gap lengths are allowed, two gaps at the ends of a polymer are transformed into one larger gap when a polymer is removed from the DNA plasmid. The new gap is always of positive length since the polymer had to be attached to the DNA with at least one monomer unit. The creation of gaps of size p due to removal is proportional to the total number of gaps of sizes q and $p-x-q$ with $1-x \le q \le P_0-1$. Thus we have a gap creation term which depends on the removal rate and applies to gaps that are at least 1-site long, namely

$$U_p^f = \frac{k_r}{M_0} \sum_{q=1-x}^{p-1} N_q N_{p-x-q}, \tag{19}$$

where k_r is the removal rate. The lower and upper limits correspond to the largest possible overlap.

When a gap of size p is destroyed by polymer removal, the removal rate is proportional to the number of such gaps; and since two gaps are destroyed when a polymer is removed, it is also dependent on the number and size of other gaps

$$U_p^r = 2\frac{k_r N_p}{M_0} \sum_{q=1-x}^{P_0-p-x} N_q. \tag{20}$$

It is possible for overlaps to overlap; this depends on the order in which adjacent polymers attach to the DNA. An example of possible overlaps is illustrated in figure 3. Polymer (b) shares an overlap of length 3 with polymer (a) and an overlap of length 4 with polymer (c); polymer (c) overlaps (a) as well as (b).

Polymer removal is modelled in a way similar to that described in Section II. The only difference is that when polymers are allowed to overlap, the smallest gap possible has length $1-x$ (corresponding to an overlap of length $x-1$). In this case our governing equations for binding and removal are

$$\frac{\mathrm{d}N_{P_0}}{\mathrm{d}t} = -F_{P_0}^r + U_{P_0}^f, \tag{21a}$$

$$\frac{\mathrm{d}N_p}{\mathrm{d}t} = F_p^f - F_p^r + U_p^f - U_p^r \quad (1 \le p \le P_0-1), \tag{21b}$$

$$\frac{\mathrm{d}N_p}{\mathrm{d}t} = F_p^{f-} + U_p^f - U_p^r \quad (2-x \le p \le 0), \tag{21c}$$

$$\frac{\mathrm{d}N_{1-x}}{\mathrm{d}t} = F_{1-x}^{f-} - U_{1-x}^r. \tag{21d}$$

B. Numerical results

As in Section II B, the overlapped binding equations were solved using a semi-implicit extrapolation method with adaptive step-size control. The charge neutralisation for typical simulations are presented in Figure 9.

The effect of polymer removal is very different when there is overlapped binding. Whereas the removal of polymers for non-overlapped simulations resulted in *higher* steady-state charge neutralisations (see Figures 7 and 8) in the overlapped case it results in a *lower* equilibrium charge neutralisation (see Figure 9).

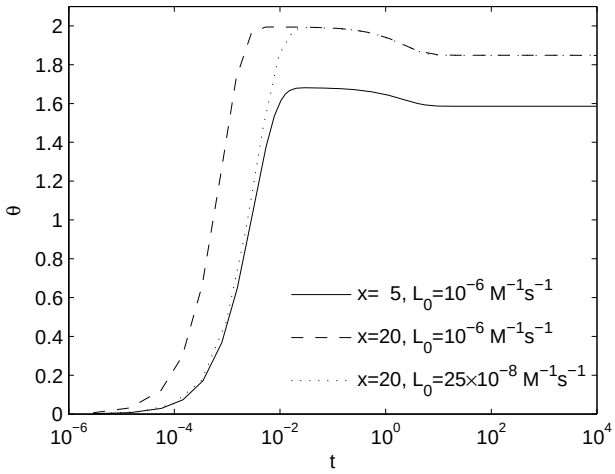

FIG. 9: Effect of polymer length on the kinetics of binding ($A_0 = 5 \times 10^{-9}$M, $P_0 = 200$ sites, $k_f = 10^8 \mathrm{M}^{-1}\mathrm{s}^{-1}$, $k_r = 0.2\mathrm{s}^{-1}$).

We note from Figure 9 that the equilibrium charge neutralisation appears to depend only on the polymer length, and is independent of polymer concentration. This is in clear contrast to the system where overlaps are prohibited (Figure 8), where charge-neutralisation depends on a complex combination of polymer concentration in the solution as well as polymer length.

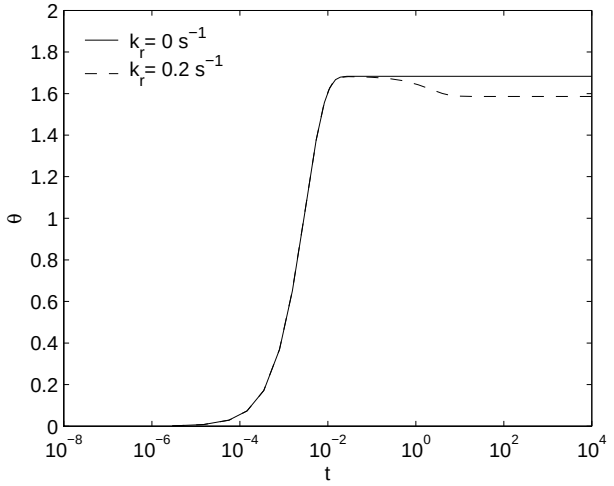

FIG. 10: Effect of removal on charge neutralisation. Parameter values: $L_0 = 10^{-6}$M, $A_0 = 5 \times 10^{-9}$M, $P_0 = 200$ sites, $x = 5$ sites, $k_f = 10^8 \mathrm{M}^{-1}\mathrm{s}^{-1}$.

The gap distributions corresponding to the equilibrium charge neutralisations of Figure 10 are presented in Fig-

ure 11. It can be seen that irreversible binding results in a uniform distribution of gap (overlap) sizes and that when removal occurs the number of gaps decreases as the gaps increase in size; that is, larger overlaps are less frequent, a similar result to that presented in Figure 5 where the incluion of removal leads to a more pronounced, size-dependent gap-distribution.

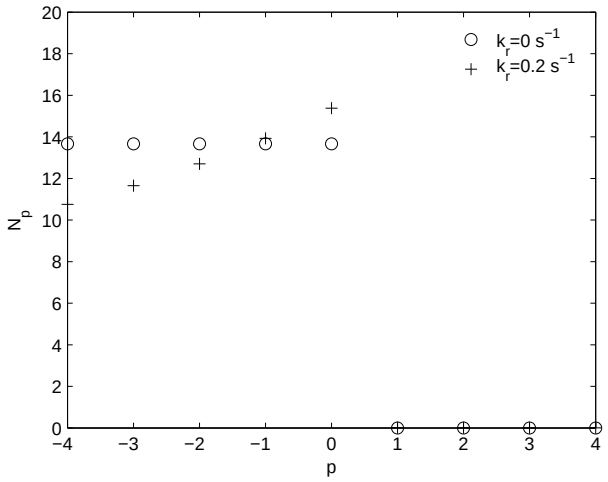

FIG. 11: Effect of removal on steady-state gap distribution ($L_0 = 10^{-6}$M, $A_0 = 5 \times 10^{-9}$M, $P_0 = 200$ sites, $x = 5$ sites, $k_f = 10^8 \mathrm{M}^{-1}\mathrm{s}^{-1}$).

Since longer polymers have more charge than their shorter counterparts, their binding rate constant may differ from those of shorter polymers. Considering only the solid and the dashed lines in Figure 9, the initial concentration of the polymers (L_0) is set to be the same in both cases. As a result there is much greater unneutralised charge of free polymers when $x = 20$ than when $x = 5$. The free polymer concentration in the solution is decreased every time one of the polymers binds to the DNA. Fewer polymers are required to cover the DNA surface if they are longer and therefore the reduction of polymer concentration in solution from $t = 0$ to equilibrium will be greater in the case of shorter polymers. The effects should be even more noticeable when the initial concentration of free polymers is small.

IV. EFFECT OF MOTION ON BINDING WITHOUT OVERLAPS

A. Modelling motion

In this section we consider the case where polymers move along the plasmid; no polymers can adhere, or be removed from the plasmid and overlapped binding cannot occur. This corresponds to (6) with $F_p = 0 = U_p$ and $V_p \neq 0$. We also assume that the initial distribution of gaps is given by $N_p(0)$. We assume that a polymer molecule can move only if it has a non-zero gap to one side of it, and that polymer motion occurs in unit steps. Figure 12 illustrates the effect of possible motions on a gap of length p.

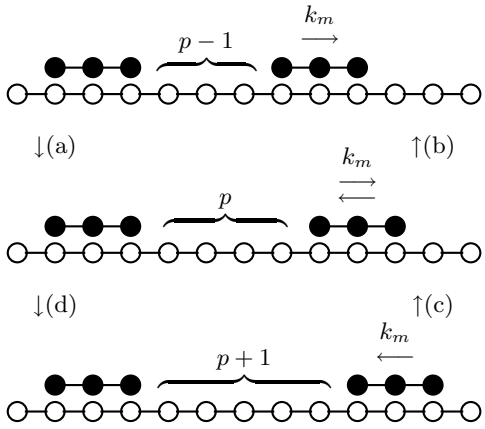

FIG. 12: Series of sketches illustrating how polymer movement can lead to the formation and destruction of a gap of length p. The processes labelled (a), (b), (c) and (d) are modelled by formulae 22(a)-(d) respectively.

The effects that polymer movement, as depicted in Figure 12, has on gap distribution are shown below

$$V_p^{f-} = k_m \underbrace{N_{p-1}\left(1 - \frac{N_0}{M_0}\right)}_{\substack{\text{gap of size} \\ p-1 \text{ grows}}}, \tag{22a}$$

$$V_p^{r-} = k_m \underbrace{N_p}_{\substack{\text{gap of size} \\ p \text{ shrinks}}}, \tag{22b}$$

$$V_p^{f+} = k_m \underbrace{N_{p+1}}_{\substack{\text{gap of size} \\ p+1 \text{ shrinks}}}, \tag{22c}$$

$$V_p^{r+} = k_m \underbrace{N_p\left(1 - \frac{N_0}{M_0}\right)}_{\substack{\text{gap of size} \\ p \text{ grows}}}, \tag{22d}$$

where k_m is the rate of polymer motion along the DNA. Superscripts + and − refer to transformations between the gap of the length p and larger and smaller gaps respectively. As before, superscripts f and r refer to gap formation and removal respectively. Gaps can grow only if there is a non-zero gap on the other side of the polymer, allowing polymer to move, hence the factor $(1 - N_0/M_0)$ in (22a) and (22d), N_0/M_0 being the probability of any given gap having size zero. Using (22) to construct gap distribution kinetics equations due to polymer motion, and combining with the effects of adhesion, removal mod-

elled by (18), we obtain

$$\frac{\mathrm{d}N_p}{\mathrm{d}t} = -F_p^r + U_p^f, \qquad (P_0 - x + 1 \le p \le P_0) \quad (23a)$$

$$\frac{\mathrm{d}N_{P_0-x}}{\mathrm{d}t} = F_{P_0-x}^f - F_{P_0-x}^r + U_{P_0-x}^f - U_{P_0-x}^r + V_{P_0-x}^{f-} - V_{P_0-x}^{r-}, \quad (23b)$$

$$\frac{\mathrm{d}N_p}{\mathrm{d}t} = F_p^f - F_p^r + U_p^f - U_p^r + V_p^{f+} + V_p^{f-} - V_p^{r+} - V_p^{r-} \qquad (x \le p \le P_0 - x - 1), \quad (23c)$$

$$\frac{\mathrm{d}N_p}{\mathrm{d}t} = F_p^f - U_p^r + V_p^{f+} + V_p^{f-} - V_p^{r+} - V_p^{r-} \qquad (1 \le p \le x - 1), \quad (23d)$$

$$\frac{\mathrm{d}N_0}{\mathrm{d}t} = F_0^f - U_0^r + V_0^{f+} - V_0^{r+}. \quad (23e)$$

B. Results for the system including adhesion, removal and motion

The evolution of the gap distributions $N_p(t)$ was calculated by solving equations (23) numerically using a special routine for stiff systems (the subroutine D02NBF of the NAG Mark 18 Fortran library). The charge neutralisation is calculated from $\theta = x(M_0 - 1)/P_0$, where M_0 is the total number of gaps.

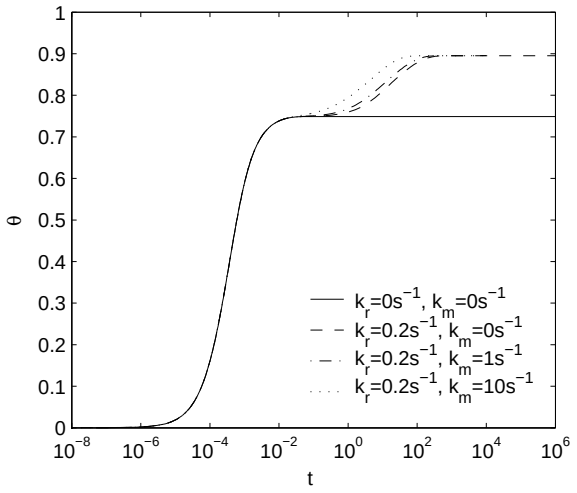

FIG. 13: Effect of polymer motion on the kinetics of charge neutralisation, θ. Parameter values: $L_0 = 10^{-6}$M, $A_0 = 2 \times 10^{-9}$M,$P_0 = 500$ sites, $x = 20$ sites, $k_f = 10^8\mathrm{M}^{-1}\mathrm{s}^{-1}$).

The kinetics of charge neutralisation for systems with different rates of polymer motion are displayed in Figure 13. Numerical simulations again show that the equilibrium charge neutralisation for systems with polymer-removal, and with or without polymer-motion are identical; the difference is that the equilibrium state is reached faster when motion is present. The equilibrium charge neutralisation for systems with motion and no removal is the same as that for the systems with removal and no motion.

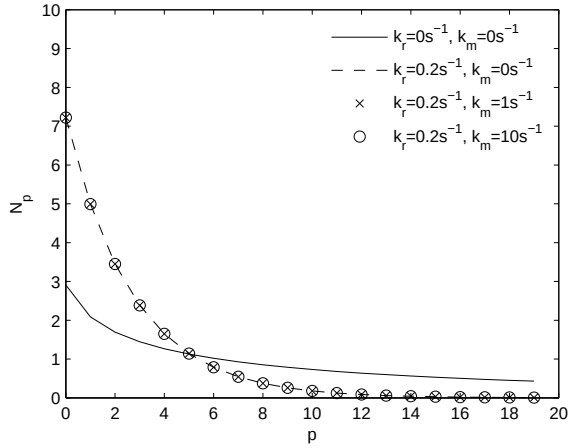

FIG. 14: Effect of polymer motion on equilibrium gap distribution, N_p. Parameter values: $L_0 = 10^{-6}$M, $A_0 = 2{\times}10^{-9}$M, $P_0 = 500$ sites, $x = 20$ sites, $k_f = 10^8\mathrm{M}^{-1}\mathrm{s}^{-1}$.

The equilibrium gap distributions corresponding to the charge neutralisation curves shown in Figure 13 are plotted in Figure 14. They show that when binding is reversible and/or when motion is included, the equilibrium distribution is identical.

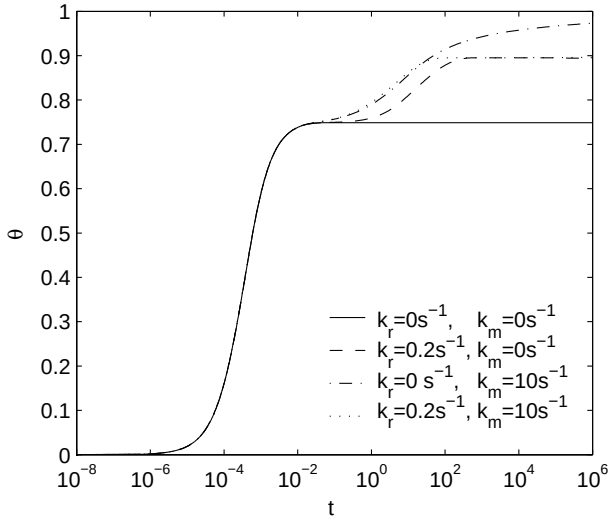

FIG. 15: Combined effects of polymer motion and removal on the kinetics of charge neutralisation. Parameter values: $L_0 = 10^{-6}$M, $A_0 = 2 \times 10^{-9}$M, $P_0 = 500$ sites, $x = 20$ sites, $k_f = 10^8\mathrm{M}^{-1}\mathrm{s}^{-1}$.

Figure 15 illustrates a situation when polymers cannot leave the DNA after they bind but can move along the DNA. The values of θ for reversible and irreversible binding with motion initially coincide. Irreversible binding (corresponding to dash-dotted line in Figure 15) ap-

proaches complete charge neutralisation ($\theta = 1$) for large times. Such behaviour is expected for any binding rate and any length of polymer since polymers simply fill all the gaps large enough to accommodate them; random polymer motion will eventually result in gaps coalescing to gaps large enough to accept further polymers until the entire DNA plasmid has been neutralised.

C. Fast motion asymptotics

An equation for charge neutralisation for cases in which polymers move along the DNA molecule at much greater rates than those at which either binding or removal occur on DNA of infinite length was derived by Epstein in [5]. In this section we use equations (23) to determine the charge neutralisation kinetics for this case, and, in so doing, confirm Epstein's results.

In the later stages of the process, when motion becomes important, only the distribution of short gaps is relevant since the large gaps will have completely disappeared.

Over short timescales, no adhesion or removal occurs, and the kinetics are governed by motion. Thus, setting $F_p = U_p = 0$ in equation (23), we have the equation for the gap-distribution on the DNA plasmid in the limit of $P_0 \to \infty$ is

$$\frac{1}{k_m}\frac{\mathrm{d}N_0}{\mathrm{d}t} = N_1 - \left(1 - \frac{N_0}{M_0}\right) N_0, \tag{24a}$$

$$\frac{1}{k_m}\frac{\mathrm{d}N_p}{\mathrm{d}t} = N_{p+1} - \left(1 - \frac{N_0}{M_0}\right) N_p - N_p + \left(1 - \frac{N_0}{M_0}\right) N_{p-1} \quad (p \geq 1), \tag{24b}$$

where $M_0 = \sum_{p=0}^{\infty} N_p$ and hence $\frac{\mathrm{d}}{\mathrm{d}t} M_0$ is an order of magnitude smaller than M_0.

At equilibrium equation (24a) implies

$$N_1 = N_0 \left(1 - \frac{N_0}{M_0}\right). \tag{25}$$

When $\dfrac{\mathrm{d}}{\mathrm{d}t} N_p = 0$, equations (24b) form a system of linear, constant coefficient, recurrence relations whose solution is given by

$$N_p(t) = N_0 \left(1 - \frac{N_0}{M_0}\right)^p, \tag{26}$$

for any choice of the parameters N_0, M_0. For a given system, M_0 should be constant over the timescale considered in (24b). This suggests that there is a two-parameter family of solutions to (24a), parametrised by N_0 and M_0, N_0 being the number of gaps of zero length and M_0 being the total number of gaps (of any size).

Assuming (26) holds for $0 \leq p \leq P_0$ and $P_0 \gg 1$, we have

$$M_1 = \frac{M_0}{N_0}\left(M_0 - N_0\right). \tag{27}$$

An expression relating the number of gaps of size zero to M_0 is found by applying the identity $P_0 - M_1 = x(M_0 - 1)$ to (27). This gives

$$N_0 = \frac{M_0^2}{P_0 + x + (1-x)M_0}. \tag{28}$$

At any particular time we expect the shape of the distribution $N_p(t)$ to be given by (26) with (28) and $0 < M_0 < 1 + P_0/x$.

Over large times $M_0(t)$ will vary as polymers slowly adhere to the DNA or are removed from it. We substitute for N_0 from (28) into (26) to get the approximate distribution for all gap sizes

$$N_p(t) = \frac{M_0^2}{P_0 + x + (1-x)M_0}\left(\frac{P_0 + x - xM_0}{P_0 + x + (1-x)M_0}\right)^p, \tag{29}$$

where the only time-dependence is via $M_0(t)$ which we determine below. Since we expect $N_p = 0$ for $p \gg x$, this will be a good approximation only in the later stages of the polymer adhesion process, where N_p is small for $p \geq x$.

We now derive an evolution equation for M_0 that is valid at large times when polymer adhesion and removal occurs. From (23) we obtain the ODE

$$\frac{\mathrm{d}M_0}{\mathrm{d}t} = \sum_{p=0}^{P_0 - x}\left(K_f(p+1)N_{p+x} - K_r N_p \sum_{q=0}^{P_0 - p - x} N_q\right). \tag{30}$$

To close the system, we substitute from (29) into (30), write $K_r = k_r/M_0$ and

$$K_f = k_f L(t) = k_f\left(L_0 - A_0(M_0 - 1)\right),$$

and set the upper limits in (30) to infinity. In this way, we obtain

$$\frac{\mathrm{d}M_0}{\mathrm{d}t} = \frac{k_f\left(L_0 - A_0(M_0-1)\right)\left(P_0 - x(M_0-1)\right)^x}{\left(P_0 - x(M_0-1) + M_0\right)^{x-1}} - k_r M_0. \tag{31}$$

Using $\theta = x(M_0 - 1)/P_0$, we rewrite this as an evolution equation for the charge neutralisation which, on taking the limit $P_0 \to \infty$, yields

$$\frac{\mathrm{d}\theta}{\mathrm{d}t} = \frac{k_f x(L_0 - A_0(M_0-1))(1-\theta)^x}{(1 - (\frac{x-1}{x})\theta)^{x-1}} - k_r\theta. \tag{32}$$

Epstein's derivation is based on the McGhee-von Hippel isotherm [25]. In [5], Epstein uses θ to denote the quantity $(M_0 - 1)/P_0$ so to convert to our charge neutralisation variable $\theta = x(M_0 - 1)/P_0$ we rescale multiply Epstein's θ by x. Equation (18) of [5] is thus transformed into (32) above.

Equation (31) is applicable to the binding of polymers that have a high rate of movement along the DNA molecule. The steady state solution of equation (31) also applies to the polymers that do not move along the DNA ($k_m = 0$) but are removable ($k_r > 0$). Numerical solutions of equation (31) are plotted in Figure 16. As expected, the steady-state charge neutralisation is the same regardless of whether the polymers move. The time taken to approach that state is considerably reduced when the polymers move. All curves display identical behaviour on the faster timescale when the binding process dominates.

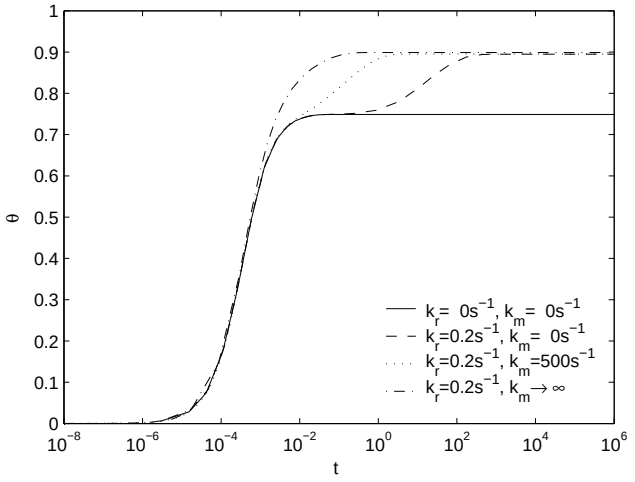

FIG. 16: Asymptotic solution of charge neutralisation kinetics ($L_0 = 10^{-6}$M, $A_0 = 2 \times 10^{-9}$M, $P_0 = 500$ sites, $x = 20$ sites, $k_f = 10^8 \mathrm{M}^{-1}\mathrm{s}^{-1}$).

We now use equation (32) to calculate two further quantities: firstly the rate at which the charge neutralisation approaches unity in the case where there is motion and no removal, and secondly the equilibrium charge neutralisation when the removal rate is small.

1. *Equilibrium charge neutralisation in the case of small removal rates*

We consider the case where the polymers are long, and the DNA plasmid is extremely long, so that it can accommodate many polymers. Thus we use the scalings $x = 1/\epsilon$ and $P_0 = y/\epsilon^2$ with $\epsilon \ll 1$. This implies that, to leading order, $M_0 = \theta/\epsilon$, and that (31) simplifies to

$$\frac{\mathrm{d}\theta}{\mathrm{d}t} = -k_r\theta + \frac{k_f}{\epsilon^2}(L_1 - A_0\theta y)(1-\theta)\exp\left(\frac{-\theta}{1-\theta}\right), \quad (33)$$

where $A_0 = O(1)$ and $L_0 \approx L_1/\epsilon$ with $L_1 = O(1)$.

As shown above, if there is motion with no removal, the equilibrium charge neutralisation is unity. However, in the case of motion with *reversible* binding, the equilibrium value of θ is below unity. To obtain an asymptotic expression for the equilibrium value when k_r is small we write $\theta = 1 - \delta$ with $\delta \ll 1$. From (33) we find that at equilibrium

$$\frac{1}{\delta}e^{1/\delta} = \frac{k_f}{k_r\epsilon^2}(L_1 - A_0 y) =: q, \quad (34)$$

and $1/\delta = W(q)$, where W is Lambert's function [26] which has the property that $W(q) \sim \log q$ for $q \gg 1$. Thus for systems with a small removal rate the equilibrium charge neutralisation is given by

$$\theta \sim 1 - \frac{1}{\log(k_f(L_1 - A_0 y)/k_r\epsilon^2)}, \quad (35)$$

or, reintroducing the scales $x = 1/\epsilon$ and $P_0 = y/\epsilon^2$,

$$\theta \sim 1 - \frac{1}{\log(k_f(L_0 x - A_0 P_0)/k_r)}. \quad (36)$$

The accuracy of this asymptotic solution is investigated in the next section.

2. *Large-time solution for the case of motion with no removal*

If there is polymer motion, but no removal then the charge neutralisation approaches exactly unity in the large-time limit. To analyse the large-time solution in this case, we return to (33) noting that $k_r = 0$. We expect $\theta \to 1$ as $t \to \infty$. The large-scale asymptotics can be derived by introducing $\psi = 1 - \theta \ll 1$ for which

$$\epsilon^2\frac{\mathrm{d}\psi}{\mathrm{d}t} = -k_f(L_1 - A_0 y)\psi\,\mathrm{e}^{-1/\psi}. \quad (37)$$

Hence we find that $\theta(t) \sim 1 - 1/\log(t)$ as $t \to \infty$, which gives the extremely slow convergence seen in the top curve of Figure 15.

D. Charge neutralisation as a function of removal rate

We now study the effect of varying the ratio of binding to removal rates on the equilibrium charge neutralisation. Steady-state solutions for reversible binding with different values of k_f/k_r are compared to irreversible binding solutions in Figure 17.

The solid line in Figure 17 represents the steady-state solution of equation (31) for various values of k_f/k_r. The dotted line corresponds to the steady-state of the irreversible binding system where it is assumed that polymers cannot leave ($k_r = 0$) or move along ($k_m = 0$) the DNA once attached. The two curves intersect when $k_f/k_r = \kappa_0 = 2.09 \times 10^6\mathrm{M}^{-1}$. The dashed line in in Figure 17 corresponds to asymptotic solution (36). We observe good agreement for $k_f/k_r > 10^6$.

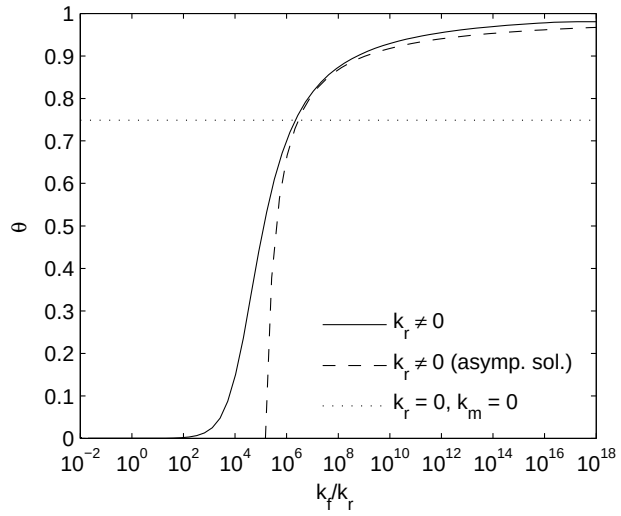

FIG. 17: Steady-state charge neutralisation calculated from numerical solution of equation (31) (solid line), asymptotic solution (36)(dashed line) and the recurrence relation [1] (dotted line). Parameter values: $L_0 = 10^{-6}$M, $A_0 = 2 \times 10^{-9}$M, $P_0 = 500$ sites, $x = 20$ sites, $k_f = 10^8 \mathrm{M}^{-1}\mathrm{s}^{-1}$.

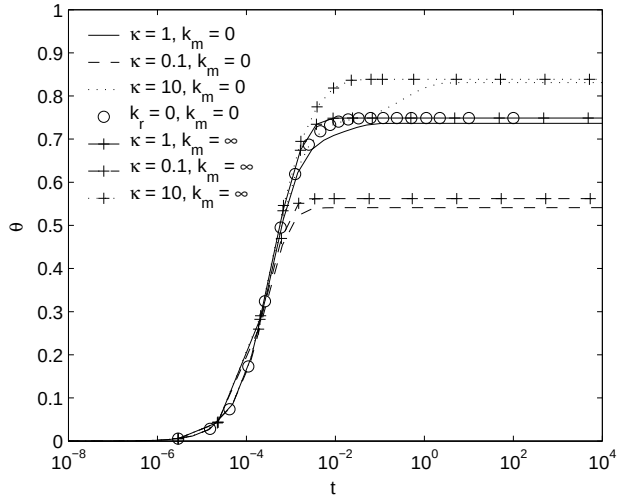

FIG. 18: Kinetics of charge neutralisation for various values of the removal rate ($L_0 = 10^{-6}$M, $A_0 = 2 \times 10^{-9}$M, $P_0 = 500$ sites, $x = 20$ sites, $\kappa = k_f/(k_r\kappa_0)$, $\kappa_0 = 2.09 \times 10^6 \mathrm{M}^{-1}$).

E. Kinetics of high removal-rate reactions

We now examine the effects of varying the removal and movement rates on charge neutralisation. Figure 18 shows the kinetics of charge neutralisation for irreversible binding (circles) together with three pairs of curves. In each pair, one curve corresponds to no motion and the other to extremely rapid motion. We define $\kappa_0 = k_f/k_r$ for the value of this ratio which gives an equilibrium charge neutralisation equal to that which occurs in the pure adhesion case ($k_r = 0 = k_m$); from the above subsection we note that $\kappa_0 = 2.09 \times 10^6$ M^{-1}. The definition of κ implies $k_f = k_r\kappa_0\kappa$ so that large values of κ represent adhesion-dominated systems whilst $\kappa < 1$ indicates that removal plays the dominant role. We specify a removal rate through κ such that $k_r = k_f/\kappa_0\kappa$, thus $\kappa = 10$ corresponds to a low removal rate, and $\kappa = 0.1$, a high removal rate.

In Figure 18, the solid line with bars across it corresponds to binding when polymers are assumed to move rapidly along the DNA plasmid ($k_m \to \infty$, $\kappa = 1$). The unmarked solid line corresponds to the reversible process when polymers do not move along the DNA plasmid ($k_m = 0$, $\kappa = 1$). Both cases with $\kappa = 1$ yield results that are very close to irreversible binding but high movement rates leads to slightly higher charge neutralisation than when $k_m = 0$.

When the removal rate is high ($\kappa = 0.1$) the charge neutralisation is low ($\theta \approx 0.55$) and again motion causes a slight increase in θ. The same qualitative behaviour is observed when the removal rate is low ($\kappa = 10$) except that the charge neutralisation is much higher ($\theta \approx 0.83$).

The results presented in Figure 18 suggest that using equation (32) to determine the steady state charge neutralisation may underestimate the correct solution when the removal rate is relatively low.

V. MODELLING MOTION WITH OVERLAPS

A. Pure motion

In this section we consider the case where a finite number of polymer molecules are attached to the DNA. The polymers can move along the plasmid,but no further polymer can adhere, and none can be removed.

We assume that the initial distribution of gaps is given by $N_p(0)$ and since overlaps are permitted, $-(x-1) \leq p \leq P_0$. We wish to determine how this distribution evolves due to the allowed motion of adhered polymer molecules. We suppose that a polymer molecule will always move unless it has reached maximum possible overlap $p = -x + 1$ on one side, and that each motion corresponds to the motion of a polymer over one lattice site. Figure 19 illustrates the range of effects that polymer movement can have on gaps of length p.

The effects that polymer movements (a)-(d) displayed

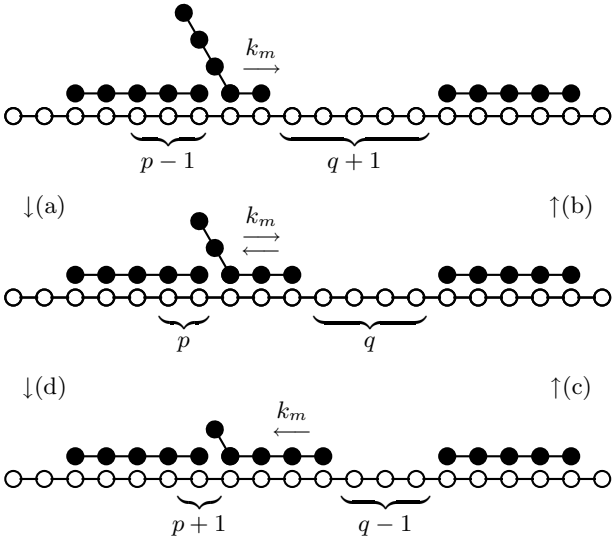

FIG. 19: Illustration of p-gap formation and destruction due to polymer motion; in this case $p < 0$ so the 'gap' is actually an overlap. The processes (a)-(d) are modelled by formulae 38(a)-(d) respectively.

in Figure 19 have on the gap distribution are shown below

$$V_p^{f-} = k_m \underbrace{\left(1 - \frac{N_{1-x}}{M_0}\right) N_{p-1}}_{\substack{\text{gap of size} \\ p-1 \text{ grows}}}, \tag{38a}$$

$$V_p^{r-} = k_m \underbrace{N_p}_{\substack{\text{gap of size} \\ p \text{ shrinks}}}, \tag{38b}$$

$$V_p^{f+} = k_m \underbrace{N_{p+1}}_{\substack{\text{gap of size} \\ p+1 \text{ shrinks}}}, \tag{38c}$$

$$V_p^{r+} = k_m \underbrace{N_p \left(1 - \frac{N_{1-x}}{M_0}\right)}_{\substack{\text{gap of size} \\ p \text{ grows}}}, \tag{38d}$$

As before, superscripts f and r refer to gap formation and removal respectively, and k_m is the rate of polymer motion along the DNA. The additional superscripts $\pm$ refer to transitions between gaps of length p and $p \pm 1$ respectively.

Using (38) to construct equations for the evolution of the gap-distribution, combining with the effects of adhesion, and removal modelled by (21), we obtain

$$\frac{\mathrm{d}N_{P_0}}{\mathrm{d}t} = -F^r_{P_0} + U^f_{P_0}, \tag{39a}$$

$$\frac{\mathrm{d}N_{P_0-1}}{\mathrm{d}t} = F^f_{P_0-1} - F^r_{P_0-1} + U^f_{P_0-1} - U^r_{P_0-1} + V^{f-}_{P_0-1} - V^{r-}_{P_0-1}, \tag{39b}$$

$$\frac{\mathrm{d}N_p}{\mathrm{d}t} = F^f_p - F^r_p + U^f_p - U^r_p + V^{f+}_p + V^{f-}_p - V^{r+}_p - V^{r-}_p \qquad (1 \le p \le P_0 - 2), \tag{39c}$$

$$\frac{\mathrm{d}N_p}{\mathrm{d}t} = F^{f-}_p + U^f_p - U^r_p + V^{f+}_p + V^{f-}_p - V^{r+}_p - V^{r-}_p \qquad (2 - x \le p \le 0), \tag{39d}$$

$$\frac{\mathrm{d}N_{1-x}}{\mathrm{d}t} = F^{f-}_{1-x} - U^r_{1-x} + V^{f+}_{1-x} - V^{r+}_{1-x}. \tag{39e}$$

B. Numerical solution for adhesion, removal and motion

As before, the evolution of the gap distributions $N_p(t)$ was calculated by solving equations (39) numerically using the subroutine D02NBF from the NAG Mark 18 Fortran library. The charge neutralisation was calculated from $\theta = x(M_0 - 1)/P_0$, where M_0 is the total number of gaps.

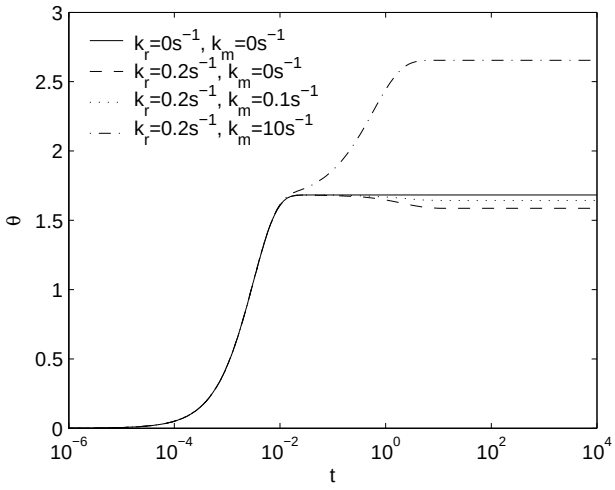

FIG. 20: Effect of polymer motion on kinetics of charge neutralisation when overlaps are permitted, log scale in time ($L_0 = 10^{-6}$M, $A_0 = 5 \times 10^{-9}$M, $P_0 = 200$ sites, $x = 5$ sites, $k_f = 10^8 \mathrm{M}^{-1}\mathrm{s}^{-1}$).

In Figure 20 we compare charge neutralisation for polymer binding with and without motion. Recall that with overlapped binding, polymer removal leads to a reduction in charge-neutralisation over larger timescales. Even a relatively slow rate of movement results in a large increase in charge neutralisation (dotted line in Figure 20)

compared to that without movement (dashed line in Figure 20). Increasing the rate of movement further results in a further increase of charge neutralisation (dash-dot line in Figure 20).

When systems allowing motion with overlaps (Figure 20) are compared with systems allowing motion without overlaps (Figure 13), it is clear that allowing overlaps leads to a further large increase in charge neutralisation. In the case of binding without overlaps movement merely resulted in a faster approach to the reversible binding equilibrium.

Further information about the system can be obtained by studying the gap distribution (see Figure 21). The data marked by x's in Figure 21 correspond to the largest movement rate, and shows a large number of overlaps of the largest possible size. Rearrangements which increase the size of overlaps when the DNA plasmid is already fully covered lead to this scenario where very large charge neutralisations observed, as shown in Figure 20, and are almost certainly unphysical. This is due to an over-simplified model of polymer-motion; a more accurate model of polymer motion would take account of a charge-charge interactions and hence favour motion which led to a reduction in overlap size.

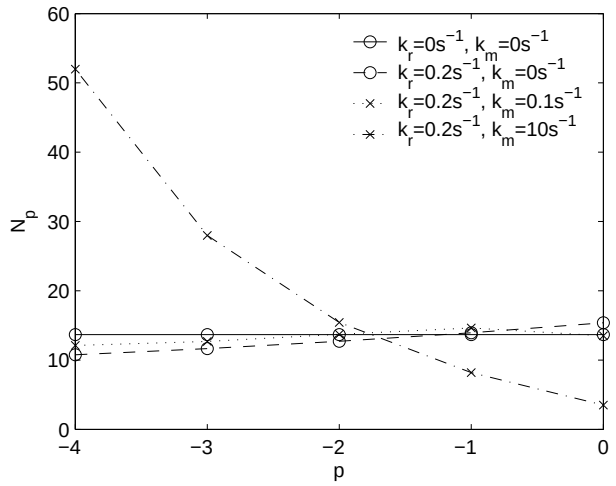

FIG. 21: Effect of polymer motion on equilibrium gap distribution, ($L_0 = 10^{-6}$M, $A_0 = 5 \times 10^{-9}$M, $P_0 = 200$ sites, $x = 5$ sites, $k_f = 10^8 \mathrm{M}^{-1}\mathrm{s}^{-1}$).

The charge neutralisation process can be limited by preventing motions that increase the number or size of existing overlaps. Removing all movement terms that lead to the formation of overlaps from equations (39) gives the more physically realistic equations

$$\frac{\mathrm{d}N_{P_0}}{\mathrm{d}t} = 0, \tag{40a}$$

$$\frac{1}{k_m}\frac{\mathrm{d}N_{P_0-1}}{\mathrm{d}t} = -N_{P_0-1}, \tag{40b}$$

$$\frac{1}{k_m}\frac{\mathrm{d}N_p}{\mathrm{d}t} = N_{p+1} - N_p \quad (P_0 - x + 1 \le p \le P_0 - 2), \tag{40c}$$

$$\frac{1}{k_m}\frac{\mathrm{d}N_{P_0-x}}{\mathrm{d}t} = N_{P_0-x+1} - N_{P_0-x} + N_{P_0-x-1}S,$$

$$\frac{1}{k_m}\frac{\mathrm{d}N_p}{\mathrm{d}t} = -N_pS + N_{p+1} - N_p + N_{p-1}S \quad (1 \le p \le P_0 - x - 1), \tag{40d}$$

$$\frac{1}{k_m}\frac{\mathrm{d}N_0}{\mathrm{d}t} = -N_0S + N_1 + N_{-1}S, \tag{40e}$$

$$\frac{1}{k_m}\frac{\mathrm{d}N_p}{\mathrm{d}t} = -N_pS + N_{p-1}S \quad (2 - x \le p \le -1), \tag{40f}$$

$$\frac{1}{k_m}\frac{\mathrm{d}N_{1-x}}{\mathrm{d}t} = -N_{1-x}S, \tag{40g}$$

where $S = \frac{1}{M_0}\sum_{q=1}^{P_0} N_q$ is the proportion of gaps which are positive in length and k_m is the rate of motion.

Charge neutralisation of the system with motion limited to reducing overlaps is shown in Figure 22. Polymer motion modelled by equations (40) neither increases the charge (as it did in Figure 20), nor results in the same charge neutralisation as irreversible binding without motion (Figure 13 in Section IV B). The graph corresponding to polymers with motion rate, $k_m = 0.1s^{-1}$ in Figure 22 shows that motion results in a slight decrease in the charge neutralisation θ with the line corresponding to $k_m = 10s^{-1}$ confirming the result with charge neutralisation decreasing a little further. The kinetics of charge neutralisation in the system with modified motion still occur on the same timescales: with binding on timescale of 10^{-3} - 10^{-2}, and rearrangements leading to reduction in θ over $t \sim 10^{-1}$ - 10^{+1}.

VI. DISCUSSION

We have developed a new deterministic model of the kinetics of gap distributions occurring when polymers bind reversibly, with or without overlaps, to DNA. We have verified that the numerical simulations agree with equivalent Monte Carlo simulations. New results confirmed that removal generally increases the charge neutralisation when polymers do not overlap and decreases it when they do. We have also determined the distribution of gaps/overlaps at equilibrium. In the non-overlapping case, introducing reversible adhesion accentuates the size-dependence of gap sizes, making smaller gaps more common and larger gaps less common than in the case of irreversible adhesion (Figure 6). When over-

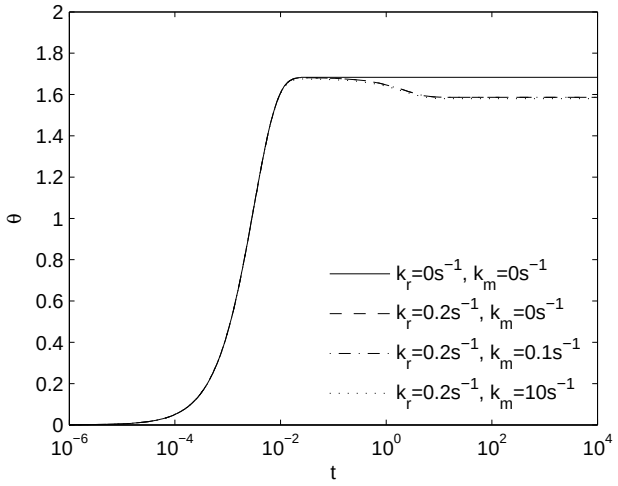

FIG. 22: Effect of limited polymer motion (40g) on the kinetics of charge neutralisation, log scale in time ($L_0 = 10^{-6}$M, $A_0 = 5 \times 10^{-9}$M, $P_0 = 200$ sites, $x = 5$ sites, $k_f = 10^8 \mathrm{M}^{-1}\mathrm{s}^{-1}$).

laps are permitted, irreversible binding produces a distribution of overlaps which is independent of size, whereas when binding is reversible small overlaps are more frequent and large gaps less common (Figure 11).

Reducing the free polymer concentration had a less pronounced effect on charge neutralisation in the case of overlapping than in the non-overlapping case. The decrease in charge neutralisation observed in non-overlapped binding with lower concentration of polymers in the solution was not observed when overlaps were allowed.

We have also extended our deterministic model to allow for polymer motion along the DNA plasmid. Numerical solutions of the non-overlapping process are in good agreement with Monte Carlo simulations and suggest that motion decreases the time taken to reach the equilibrium charge neutralisation.

Polymer motion in the overlapped system can have a dramatic effect on the equilibrium charge neutralisation. Our initial model of polymer motion allows polymers to move towards and over each other until they form the maximum possible overlap, this leads to a greatly increased equilibrium charge neutralisation, through an effect which we believe is unphysical. Although other authors have commented on the possibility of such large charge inversions [27], in many systems we believe there will be an upper limit to observed charge inversions, as noted by Tanaka & Grosberg [28]. Hence, we have proposed a modified model in which polymer-motion can only decrease overlap size. The corresponding equilibrium charge neutralisation is decreased.

We have considered one asymptotic domain in more detail, namely the case of long polymers (of length $x = 1/\varepsilon$ with $\varepsilon \ll 1$) and very long DNA plasmids (of length $P_0 = \mathcal{O}(1/\varepsilon^2)$). In the case of reversible binding without overlaps we have determined numerically how the ratio (k_f/k_r) influences the equilibrium charge neutralisation, in particular we have found an asymptotic approximation which is valid when k_f/k_r is large. Our model is based on the theory of random sequential adsorption (RSA), an approach which has been widely used previously to analyse the geometric effects of binding and blockage of binding of polymers to a DNA plasmid. The novel aspects we have introduced here are the combination of reversible adhesion and motion of the polymers along the plasmid. In Section IV C we have used asymptotic analysis to show that the system exhibits extremely slow kinetics in its approach to equilibrium.

Future work could be directed at deriving more refined formulae for the adhesion and removal rates' and their dependence on electrostatic DNA-polymer interactions. The resulting models would then be more consistent with the electrostatic/thermodynamic models of [29]. In a future paper we address DNA-polymer interactions in which the polymers have a polydisperse distribution of lengths [31, 32].

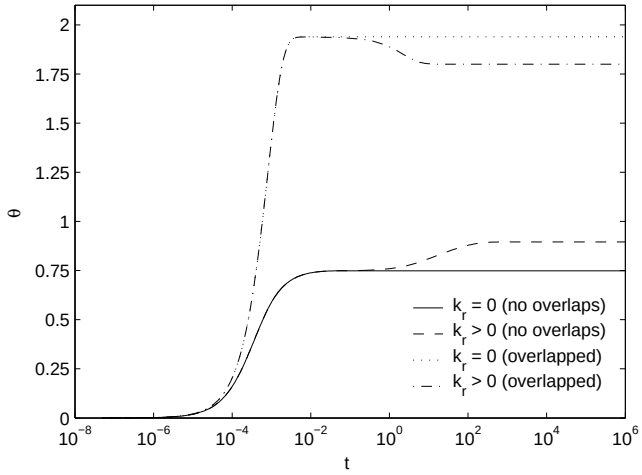

FIG. 23: Illustration of the main qualitative features of the charge neutralisation kinetics of various models of polymer binding.

In summary, our analysis of the kinetics of charge neutralisation reveals four qualitatively different types of behaviour; (see Figure 23). The simplest model of irreversible binding without overlaps predicts a one-step monotonic increase in the charge neutralisation (solid line in Figure 23). This is always insufficient to cause DNA condensation regardless of the length of the polymer as it is below the 90% needed to condense DNA (Wilson & Bloomfield [30]). When binding is reversible and without overlaps (dashed line) the dynamics exhibit a two-step monotonic increase to a higher equilibrium charge neutralisation. The counterintuitive result that including polymer-removal causes an increase in charge neutralisation is due to the fact that removal creates gaps large enough for a greater number of polymers to bind to the DNA. Irreversible binding with overlaps (dotted line

in Figure 23) exhibits the same one-step monotonic increase as irreversible binding without overlaps but leads to a much higher charge neutralisation ($\theta > 1$). The approach to the equilibrium charge neutralisation is non-monotonic when there is reversible binding with overlaps. These four types of behaviour discussed above could be matched to experimental data to predict which of the mechanisms present in our family of models of polymer-binding are relevant for a particular system.

Acknowledgements

We are grateful to Snow Stolnik and Clive Roberts for useful discussions regarding modelling and parameter values. EM was sponsored by the UK BBSRC.

[1] E Maltsev, JAD Wattis & HM Byrne. DNA charge neutralisation by linear polymers: irreversible binding. *Phys Rev E*, **74**, 011904, (2006). Also in *VJ Biol Res*, **12**, `www.vjbio.org`, (2006).

[2] A Rényi. On a one-dimensional problem concerning random space-filling. *Publ Math Inst Hung Acad Sci*, **3**, 109–127, (1958).

[3] B Bonnier, D Boyer & P Viot. Pair correlation function in random sequential absorption process", *J. Phys. A: Math. and Gen*, **27**, 3671–3682, (1994).

[4] IR Epstein. Kinetics of large-ligand binding to one-dimensional lattices: theory of irreversible binding. *Biopolymers*, **18**, 765–788, (1979).

[5] IR Epstein. Kinetics of nucleic acid-large ligand interactions: exact Monte-Carlo treatment and limiting cases of reversible binding. *Biopolymers*, **18**, 2037–2050, (1979).

[6] D Porschke. Dynamics of DNA condensation. *Biochemistry*, **23**, 4821-4828, (1984).

[7] AU Bielinska, C Chen, J Johnson, JR Baker Jr. DNA complexing with polyamidoamine dendrimers: implications for transfection. *Bioconjugate Chemistry*, **10**, 843–850, (1999).

[8] J Talbot, G Tarjus, PR van Tassel & P Viot. From car parking to protein adsorption: an overview of sequential adsorption processes. *Colloids and Surfaces A: Physicochemical and Engineering Aspects*, **165**, 287–324, (2000).

[9] E Ben-Naim & PL Krapivsky. On irreversible deposition of disordered substrates. *J Phys A; Math Gen*, **27**, 3575–3577, (1994).

[10] PL Krapivsky & E Ben-Naim. Collective properties of adsorption-desorption processes. *J Chem Phys*, **100**, 6778–6782, (1994).

[11] LR Brewer, M Corzett & R Balhorn. Protamine-induced condensation and decondensation of the same DNA molecule. *Science*, **286**, 120–123, (1999).

[12] LR Brewer, M Corzett, EY Lau & R Balhorn. Dynamics of protoamine 1 binding to single DNA molecule. *J Biol Chem*, **278**, 42403–42408, (2003).

[13] MA Lever, JPH Th'ng, X Sun & MJ Hendzel. Rapid exchange of histone H1.1 on chromatin in living human cells. *Nature*, **408**, 873–876, (2000).

[14] G Tarjus, P Schaaf & J Talbot. Generalized random sequential adsorption. *J Chem Phys*, **93**, 8352–8360, (1990).

[15] JW Evans. Random and cooperative sequential adsorption: exactly solvable problems on 1D lattices, continuum limits, and 2D extensions. In Nonequilibrium Statistical Mechanics in One Dimension, ed V Privman, CUP, (1997), (ISBN 052101834X).

[16] M Barma. Deposition-evaporation dynamics: jamming, conservation laws and dynamical diversity. In Nonequilibrium Statistical Mechanics in One Dimension, ed V Privman, CUP, (1997), (ISBN 052101834X).

[17] PR van Tassel, G Tarjus & P Viot. A kinetic model of partially reversible protein adsorption. *J Chem Phys*, **106**, 761–770, (1997).

[18] VB Teif. Ligand-induced DNA condensation: choosing the model. *Biophys J*, **89**, 2574–2587, (2005).

[19] AY Grosberg, TT Nguyen & BI Shklovskii. Colloquium: the physics of charge inversion in chemical and biological systems. *Rev Mod Phys*, **74**, 329–345, (2002).

[20] GS Manning. The molecular theory of polyelectrolyte solutions with applications to the electrostatic properties of polynucleotides. *Quarterly Review of Biophysics*, **2**, 179–246, (1979).

[21] I Rouzina & VA Bloomfield. Influence of ligand spatial organization on competitive electrostatic binding to DNA. *J Phys Chem*, **100**, 4305-4313, (1996).

[22] ER Cohen & H Reiss. Kinetics of reactant isolation. I. one-dimensional problems. *J Chem Phys*, **38**, 680–691, (1962).

[23] BJ Rackstraw, AL Martin, S Stolnik, CJ Roberts, MC Garnett, MC Davies & SJB Tendler. Microscopic investigations into PEG-cationic polymer-induced DNA condensation. *Langmuir*, **17**, 3185–3193, (2001).

[24] WH Press, SA Teukolsky, WT Vetterling & BP Flannery. Numerical Recipes in Fortran 90. The Art of Parallel Scientific Computing. Cambridge University Press", Volume 2, (1996).

[25] JD McGhee & PH von Hippel. Theoretical aspects of DNA-protein interactions: co-operative and non-co-operative binding of large ligands to a one-dimensional homogeneous lattice. *J Mol Biol*, **86**, 469–489, (1974).

[26] EW Weisstein. Lambert W-Function. From MathWorld–A Wolfram Web Resource. `http://mathworld.wolfram.com/LambertW-Function.html` (2005).

[27] TT Nguyen, AY Grosberg & BI Shklovskii. Macroions in salty water with multivalent ions: giant inversion of charge. *Phys Rev Lett*, **85**, 1568–1571, (2000).

[28] M Tanaka & AY Grosberg. Giant charge inversion of a macroion due to multivalent counterions: molecular dynamics study. *J Chem Phys*, **115**, 567–574, (2001).

[29] I Rouzina & VA Bloomfield. Competitive elecrostatic binding of charged ligands to polyelectrolytes: planar and cylindrical geometries. *J Phys Chem*, **100**, 4292–4304, (1996).

[30] RW Wilson & VA Bloomfield. Counterion-induced condensation of Deoxyribonucleic acid, a light-scattering study. *Biochemistry*, **18**, 2192–2196, (1979).

[31] E Maltsev, JAD Wattis & HM Byrne. DNA charge neutralisation by linear polymers III: mixed polymers. *preprint*, (2006).

[32] E Maltsev. Mathematical Modelling of DNA Condensation. PhD Thesis, University of Nottingham, (2005).